The Impact of Electric Vehicles Aggregator on the Stability Region of Micro-Grid System with Communication Time Delay

Hakan Gündüz, Şahin Sönmez and Saffet Ayasun
Department of Electrical and Electronics Engineering
Niğde Ömer Halisdemir University
Niğde, Turkey
hakangunduz@ohu.edu.tr, sahinsonmez@ohu.edu.tr and sayasun@ohu.edu.tr

***Abstract*—This paper investigates the impact of Electric Vehicles (EVs) on the stability region of micro-grid (MG) system with constant communication delays. A simple and efficient graphical method based on extracting the boundaries of stability regions is used to compute all stabilizing values in proportional-integral (PI) parameters space for a specified time delay. Verification of theoretical stability region boundaries is shown by time-domain simulations for test points selected from stability regions. Results show that the size of stability regions gets larger with the integration of EVs into the MG system, indicating that the stability of the MG system is improved.**

***Index Terms*--Electric vehicle, micro-grid system, stability region, time delay.**

I. INTRODUCTION

The study deals with computation of all stabilizing proportional-integral (PI) controller gains described as a region in the controller parameter space for a micro-grid (MG) system enhanced by electrical vehicles (EVs). Recently, EVs have become the focus of interest in many researches due to growing environmental pollutions, gradually depletion of fossil fuels and intermittent renewable energy sources such as PV solar and wind power [1]. EVs could be utilized in a wide range of applications such as smoothing of renewable energy sources [2], [3] and frequency regulation using vehicle-to-grid techniques [4]-[8]. Fast power output of EV batteries and thereby the fast response characteristic provides that MG systems achieve a good dynamic performance. EVs can be used as generators or loads and hence reduce generation/demand fluctuations, and improve frequency response [9]. For practical participation of EVs in frequency regulation market, a new entity called as EVs aggregator is required to aggregate and control large number of EVs in order to satisfy the frequency regulation criteria [10]-[12]. The main function of an EVs aggregator is to receive and send information about the EVs status to Load Frequency Control (LFC) center and reallocate the control signals to disperse EVs.

A MG system contains several distributed and interconnected generator units, loads and possibly energy storage units. From the grid side of the power system, micro-grid systems are regarded as a group of controllable generators and loads. They include different types of micro-sources such as micro-turbine, wind turbine, solar PV panel, and fuel cell, etc. The load generally consists of residential load or small-scale industrial loads [13], [14]. In MGs, because of continuous changes in load demand, the control of power generation is required to keep the frequency constant. The LFC strategies used in high voltage interconnected power system over the years [15] have been effectively utilized in frequency regulation of MGs [16]-[19]. In MGs, all distributed generators should be operated and controlled cooperatively to ensure a stable operation with a desirable frequency and voltage profile in the system. For that purpose, a micro-grid central controller (MGCC) is implemented together with a communication network. The main functions of MGCC are to obtain measurement and control information from local controllers, to monitor the system integrity and to decide and implement necessary control actions for regulating frequency and voltage [20]. MGs require an open and distributed communication network to receive measurement signals and to send control signals from MGCC to local controllers. Because of any disturbance on the system operation such as sudden load demand changes and unexpected fluctuations in the renewable energy source, measured signals are transmitted to MGCC through a communication infrastructure in order to restore the balance between the generation and the demand. Then, the control signals are transmitted to both local controller of micro-turbine and an EVs aggregator from MGCC. The use of such communication infrastructure causes significant amount of time delays that evidently reduce the controller performance and adversely affect the dynamics of MGs [19], [21]-[23].

978-1-5386-4722-6/19/$31.00 ©2019 IEEE

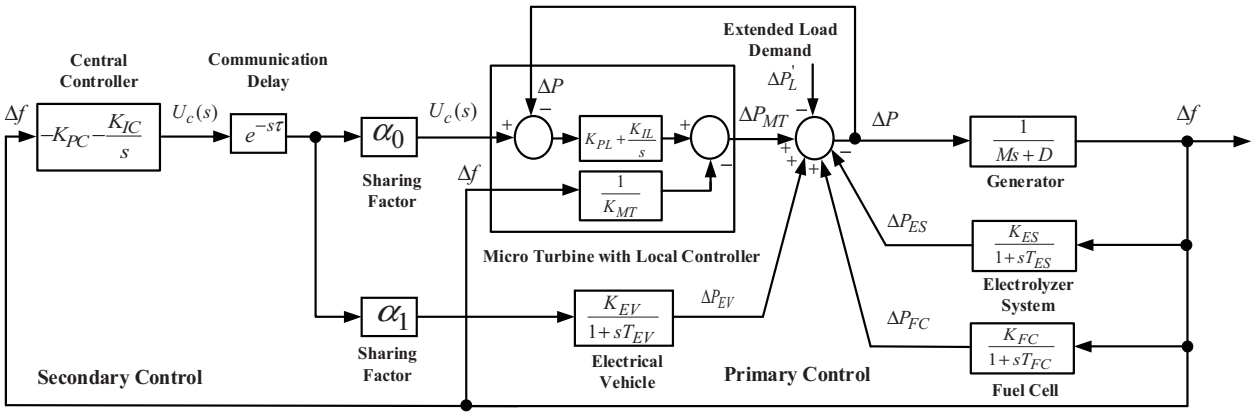

Figure 1. The time delayed micro-grid model with an EV aggregator.

EVs could be effectively used for not only frequency regulation but also for improving stability of MG systems when inevitable communication time delays are observed. The literature on the stability of time-delayed MG with an EV aggregator mainly focus on the computation of stability delay margin for a given set of PI controllers using time-domain approach based on linear matrix inequalities and Lyapunov Stability Theory [23]. However, the main drawback of that approach is that one needs to determine the delay margin and check the stability whenever the PI controller gains are changed or re-tuned, causing time-consuming stability checks. In order to avoid such a time-consuming stability check and thereby to save controller tuning time, it is necessary to determine all possible values of PI controller parameters that ensure a stable operation when a finite time delay is observed in the MG system with EVs.

The purpose of this paper is to determine the qualitative impact of EVs on the stability of MGs. For this purpose, the conventional MG system is enhanced by the integration of a group of EVs called as EVs aggregator, as illustrated in Fig. 1. In order to evaluate the impact of EVs, we need determine all possible values of PI controller parameters that ensure a stable operation when a time delay is observed. In our earlier study reported in [22], a graphical method proposed in [24], [25] has been effectively used to obtain stability regions in the PI controller parameters space for a given time delay using stability boundary locus in traditional time-delayed MG systems not including EV aggregator. This paper implements the same graphical method to determine the stability region of MG system enhanced by EVs. For different participation levels of EVs to the frequency regulation, stability regions are obtained in PI controller parameters space. The results indicate that the size of the stability region increases as the contribution of EVs to the frequency regulation increases. Finally, the accuracy of region boundaries is validated using time-domain simulations.

II. System Model

The traditional MG systems might have a poor dynamic frequency regulation performance due to intermittent renewable energy sources. EVs having fast dynamic response improve dynamical performance of the MG systems and play an important role to regulate the system frequency. Because of any disturbance on the system operation, MGCC control commands are send to both micro-turbine side and EVs aggregator side to restore system frequency. The power required to regulate the frequency is shared between EVs aggregator and micro-turbine according their participation ratios.

A. Electric Vehicle

The dynamic model of an EV battery system is usually first-order transfer function as follows [8], [12], [23]:

$$G_{EV} = \frac{\Delta P_{EV}}{U_C(s)} = \frac{K_{EV}}{1 + sT_{EV}} \tag{1}$$

where, K_{EV} and T_{EV} represent gain and time constant of the EVs battery system, respectively. In Fig. 1, the micro turbine and EVs aggregator have participation ratios of α_0 and α_1 which are allocated the participating in frequency regulation service. For example, $\alpha_0 = 1$ means that the micro-turbine is totally employed to regulate the system frequency in secondary control loop. Note that total amount of α_0 and α_1 is equal to one and is also total contribution of both generation units for frequency regulation service in the secondary control loop.

B. Micro-Grid System with EVs Aggregator

The block diagram of the traditional MG system including EV aggregators with time delay is given in Fig. 1. Note that the traditional MG system is modified to include an EV aggregator and communication time delay in Fig. 1. The parameters in Fig. 1, K_{MT}, K_{PL}, K_{IL}, K_{FC} and K_{ES} represent drop characteristics and local PI controller gains of the micro-turbine, gains of the fuel-cell and electrolyser, respectively. Moreover, T_{FC}, T_{ES}, M and D denote time constants of the fuel-cell and electrolyser, the generator inertia constant and damping coefficient, respectively. $\Delta f(s)$, $U_c(s)$, ΔP_{MT}, ΔP_{FC}, ΔP_{ES} and ΔP_{EV} are the frequency deviation, MGCC output, changes in the output power of the micro-turbine, the fuel-cell, the electrolyser and electric vehicle, respectively.

The function of the MGCC as a secondary frequency controller, which is a PI controller, is to regulate the participation ratios of micro-turbine and EVs aggregator, and to set the real power reference for the local controller of micro-turbine. The MGCC is given as follows:

$$G_{CC}(s) = K_{PC} + \frac{K_{IC}}{s} \tag{2}$$

where K_{PC} and K_{IC} are the gains of MGCC PI controller.

Observe that total time delays are lumped into a single constant delay to simplify stability analysis and is introduced by an exponential block $e^{-s\tau}$, where τ is the constant time delay that describes the total communication delay for measuring signals and control signals in the MG system with EVs. In Fig. 1, the extended load demand, which is physical signal $\Delta P_L'$, consists of housing load, wind power and PV generation, and is described as

$$\Delta P_L' = \Delta P_{HL} - \Delta P_{solar} - \Delta P_{wind} \tag{3}$$

It must be mentioned that dynamics of PV and wind power generations are not considered in the model in this study. The uncertainties of PV and wind power generations are included in the model to take into account random fluctuations observed in renewable energy sources. As illustrated in Fig. 1, PV and wind power generations are modelled as constant negative loads and included in the extended load demand in (3). For this reason, their uncertainties just represent small variations in the extended load demand. Therefore, the characteristic equation and the closed-loop stability of the time-delayed micro-grid system do not depend on the variations of PV and wind power generations and such uncertainties do not affect stability regions. The random fluctuations in the load demand, PV and wind power generations are model with a standard deviation [21], [22].

$$dP_{load} = 0.6\sqrt{P_{HL}},\ dP_{wind} = 0.8\sqrt{P_{wind}},\ dP_{solar} = 0.7\sqrt{P_{solar}} \tag{4}$$

The variations in wind, PV and housing load demand are simulated in Matlab/Simulink [26] by multiplying the random fluctuation of output power with its corresponding standard deviations.

For stability analysis, it is necessary to obtain the characteristic equation of time-delayed MG system including EVs aggregator. The characteristic equation is obtained as:

$$\begin{aligned}&\Delta(s,\tau) = P(s) + Q(s)e^{-s\tau} = 0\\ &\Delta(s,\tau) = p_6 s^6 + p_5 s^5 + p_4 s^4 + p_3 s^3 + p_2 s^2 + p_1 s\\ &+\left(q_5 s^5 + q_4 s^4 + q_3 s^3 + q_2 s^2 + q_1 s + q_0\right)e^{-s\tau} = 0\end{aligned} \tag{5}$$

The coefficients of $P(s)$ and $Q(s)$ polynomials in terms of system parameters are given in Appendix.

III. Computation of Stability Regions

To identify the boundary of the stability region for a given time delay τ, we substitute $s = j\omega_c$ and $\omega_c > 0$ into the characteristic equation in (5) and separate MGCC gains, K_{PC} and K_{IC} as follows:

$$\begin{aligned}&\Delta(s,\tau) = P(s) + Q(s)e^{-s\tau} = 0,\\ &\Delta(j\omega_c,\tau) = P(j\omega_c) + \begin{pmatrix}K_{PC}M(j\omega_c) +\\ K_{IC}N(j\omega_c)\end{pmatrix}e^{-j\omega_c\tau} = 0,\\ &\Delta(j\omega_c,\tau) = p_6(j\omega_c)^6 + p_5(j\omega_c)^5 + p_4(j\omega_c)^4\\ &\quad + p_3(j\omega_c)^3 + p_2(j\omega_c)^2 + p_1(j\omega_c)\\ &+\left[\begin{array}{l}K_{PC}\begin{pmatrix}m_5(j\omega_c)^5 + m_4(j\omega_c)^4 + m_3(j\omega_c)^3\\ +m_2(j\omega_c)^2 + m_1(j\omega_c)\end{pmatrix}\\ +K_{IC}\begin{pmatrix}n_4(j\omega_c)^4 + n_3(j\omega_c)^3 + n_2(j\omega_c)^2\\ +n_1(j\omega_c) + n_0\end{pmatrix}\end{array}\right]e^{-j\omega_c\tau} = 0.\end{aligned} \tag{6}$$

The corresponding m and n coefficients are given in Appendix.

Substituting $e^{-j(\omega\tau)} = \cos(\omega\tau) - j\sin(\omega\tau)$ into (6) and separating into the real and imaginary parts, we get a more compact form of (6) as

$$\begin{aligned}&\Delta(j\omega_c,\tau) = K_{PC}A_1(\omega_c) + K_{IC}B_1(\omega_c) + C_1(\omega_c)\\ &+j\left[K_{PC}A_2(\omega_c) + K_{IC}B_2(\omega_c) + C_2(\omega_c)\right] = 0,\\ &\Delta(j\omega_c,\tau) = \Re\left\{\Delta(j\omega_c,\tau)\right\} + j\Im\left\{\Delta(j\omega_c,\tau)\right\} = 0\end{aligned} \tag{7}$$

The expressions for A_1, B_1, C_1, A_2, B_2, and C_2 are given in Appendix. Setting both real and imaginary parts of $\Delta(j\omega_c,\tau) = 0$ in (7) to zero, we get

$$\begin{aligned}K_P A_1(\omega_c) + K_I B_1(\omega_c) + C_1(\omega_c) = 0\\ K_P A_2(\omega_c) + K_I B_2(\omega_c) + C_2(\omega_c) = 0\end{aligned} \tag{8}$$

We then solve (8) for (K_{PC}, K_{IC}) to identify the stability boundary locus $\ell(K_{PC}, K_{IC}, \omega_c)$ in the (K_{PC}, K_{IC})-plane.

$$\begin{aligned}K_{PC} &= \frac{B_1(\omega_c)C_2(\omega_c) - B_2(\omega_c)C_1(\omega_c)}{A_1(\omega_c)B_2(\omega_c) - A_2(\omega_c)B_1(\omega_c)}\\ K_{IC} &= \frac{A_2(\omega)C_1(\omega) - A_1(\omega)C_2(\omega)}{A_1(\omega_c)B_2(\omega_c) - A_2(\omega_c)B_1(\omega_c)}\end{aligned} \tag{9}$$

It should be noticed that the line $K_{IC} = 0$ is also in the boundary locus because a real root of $\Delta(j\omega_c,\tau) = 0$ in (7) could cross the imaginary axis at $s = j\omega_c = 0$ for $K_{IC} = 0$. Consequently, the boundary locus, $\ell(K_{PC}, K_{IC}, \omega_c)$ and the

line $K_{IC}=0$ split (K_{PC},K_{IC})-plane into stable and unstable regions. This part of the boundary locus is called as the Real Root Boundary (RRB) and the one obtained from (9) is defined as the Complex Root Boundary (CRB) of the stability region [22], [24], [25].

IV. RESULTS

The section presents effect of EVs with a participation ratio on the stability regions. Parameters of the micro-grid system with EV are as follows [22]:

$$M=10;\ D=1;\ K_{MT}=0.04;\ K_{FC}=1;\ T_{FC}=4;$$
$$K_{ES}=1;\ T_{ES}=1;\ K_{PL}=1;\ K_{IL}=1;\ K_{EV}=1;\ T_{EV}=0.1$$

The time delay is chosen as $\tau=2\,s$ and the crossing frequency is selected in the range of $\omega\in[0,4.0]$ rad/s for stability boundary locus. Our main purpose is to determine (K_{PC},K_{IC}) such that the characteristic equation of (5) should be Hurwitz stable. We choose participation ratios as $(\alpha_0=1,\ \alpha_1=0)$, $(\alpha_0=0.8,\ \alpha_1=0.2)$ and $(\alpha_0=0.5,\ \alpha_1=0.5)$ and determine the stability boundary locus (SBL) using (9). The corresponding three stability regions are presented in Fig. 2 and labelled as R1, R2, and R3, respectively. The stability region R1 represents all PI controller gains that guarantee the stability of MG system when the EVs aggregator is not included, $(\alpha_0=1,\ \alpha_1=0)$. The region R2 indicates the size of the stability region increases as compared with R1 when the control effort is shared by the micro-turbine and EVs aggregator. The region R3 illustrates that the region even gets larger when the contribution of EVs to the frequency regulation is further increased. These stability regions clearly show that the integration of EVs into the frequency regulation significantly improves the stability of MG systems.

The theoretical results are verified by time-domain simulations using Simulink [26]. Fig. 3 illustrates frequency deviation responses for three different controller gains of the MG system without EVs $(\alpha_0=1,\alpha_1=0)$. For $(K_{PC}=20.01,K_{IC}=6)$ inside the R1 region, the MG system without EVs is stable due to decaying oscillations. For $(K_{PC}=20.01,K_{IC}=7.135)$ on the stability boundary locus of region R1, a pair of complex conjugate roots will be located on the $j\omega$-axis and the system will be marginally stable due to sustained oscillations in the frequency response. For $(K_{PC}=20.01,K_{IC}=8)$ outside the R1 region, it is clear from Fig. 3 that the MG system is unstable due to growing oscillations.

Fig. 4 shows the effect of EVs on frequency response of the system. In order to emphasize the effect of the EVs, a test point outside R1 region and inside R2 and R3 regions $(K_{PC}=20.01,K_{IC}=8)$ is selected with the following participation ratios of $(\alpha_0=1,\alpha_1=0)$, $(\alpha_0=0.8,\alpha_1=0.2)$, and $(\alpha_0=0.5,\alpha_1=0.5)$, respectively. It is clear from Fig. 3 that the MG system without EVs is unstable for $(K_{PC}=20.01,K_{IC}=8)$ outside the R1 region. However, it is illustrated from Fig. 4 that the system is stable for $(K_{PC}=20.01,K_{IC}=8)$ when EVs aggregator with the specified participation ratios, $\alpha_1=0.2$ and $\alpha_1=0.5$ is introduced to the MG system. This result exhibits that EVs improve performance response and stability of MG system.

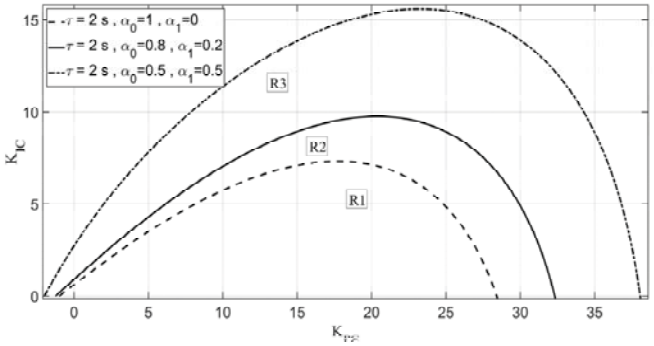

Figure 2. Stability regions for $\tau=2\,s$, $(\alpha_0=1,\alpha_1=0)$, $(\alpha_0=0.8,\alpha_1=0.2)$ and $(\alpha_0=0.5,\alpha_1=0.5)$.

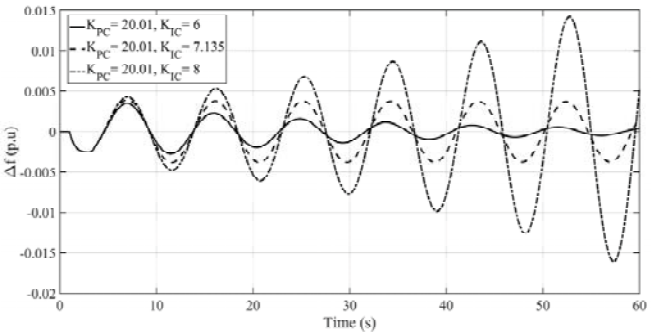

Figure 3. Frequency deviation responses for different PI controller values in R1 region.

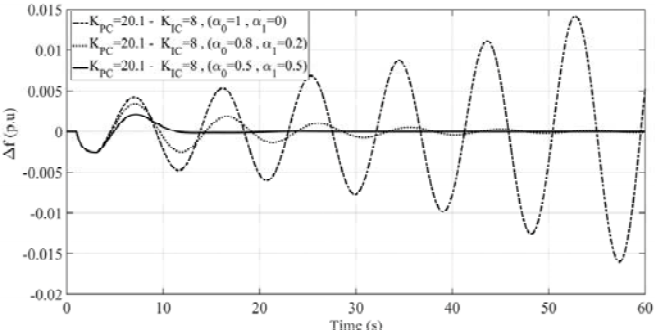

Figure 4. Frequency deviation responses for $(K_{PC}=20.01,K_{IC}=8)$ and different participation ratios.

V. CONCLUSION

This paper has investigated the stability of a time-delayed MG system that contains an EV aggregator. A graphical method based on extracting the boundaries of stability regions has been proposed to compute the stability regions. The accuracy of stability region results is proved by time-domain simulation capabilities of Matlab/Simulink. Results indicate that the EVs scheme compared to the traditional time delayed MG system not including EVs improves frequency response for different participation ratios. EVs participation ratios have a key factor on the stability regions. In the future, the gain and phase margins will be taken into account for obtaining stability regions of MG systems with multiple EVs aggregators and time delays.

REFERENCES

[1] W. Kempton and S. Letendre, "Electric vehicles as a new power source for electric utilities," *Transp. Res. Part D*, vol. 2, pp.157-175. Sep. 1997.

[2] X. Luo, S. W. Xia, and K. W. Chan, "A decentralized charging control strategy for plug-in electric vehicles to mitigate wind farm intermittency and enhance frequency regulation," *J. Power Sources*, vol. 248, pp. 604–614, Feb. 2014.

[3] J. A. Peças Lopes, P. M. Rocha Almeida, and F. J. Soares, "Using vehicle to grid to maximize the integration of intermittent renewable energy resources in Islanded electric grids," in *Proc. Int. Conf. Clean Electr. Power Renew. Energy Res. Impact*, pp. 290–295, Capri, Italy, Jun. 2009.

[4] H. Liu, Z. C. Hu, Y. H. Song, and J. Lin, "Decentralized vehicle-to-grid control for primary frequency regulation considering charging demands," *IEEE Trans. Power Syst.*, vol. 28, pp. 3480–3489, Aug. 2013.

[5] T. Masuta and A. Yokoyama, "Supplementary load frequency control by use of a number of both electric vehicles and heat pump water heaters," *IEEE Trans. Smart Grid*, vol. 3, pp. 1253–1262, Sep. 2012.

[6] J. Pillai and B. Bak-Jensen, "Integration of vehicle-to-grid in the western Danish power system," *IEEE Trans. Sustain. Energy*, vol. 2, pp. 12-19, Jan. 2011.

[7] Y. Mu, J. Wu, J. Ekanayake, N. Jenkins, and H. Jia, "Primary frequency response from electric vehicles in the Great Britain power system," *IEEE Trans. Smart Grid*, vol. 4, pp. 1142-1150, June 2013.

[8] K. S. Ko and D. K. Sung, "The effect of EV aggregators with time-varying delays on the stability of a load frequency control system," *IEEE Trans. Power Syst.,* vol. 33, pp. 669-679, Jan. 2018.

[9] M. H. Khooban, T. Niknam, F. Blaabjerg and T. Dragicevic "A new load frequency control strategy for micro-grids with considering electric vehicles," *Electr. Power Syst. Res*., vol. 143, pp. 585-598, February 2017.

[10] S. Han, S. Han, and K. Sezaki, "Development of an optimal vehicle-to-grid aggregator for frequency regulation," *IEEE Trans. Smart Grid*, vol. 1, pp. 65-72, June 2010.

[11] R. J. Bessa and M. A. Matos, "The role of an aggregator agent for EV in the electrical market," in Proc. *7th Mediterranean Conference and Exhibition on Power Generation, Transmission, Distribution and Energy Conversion*, pp. 1-9, Agia Napa, Cyprus, Nov. 07-10, 2010.

[12] H. Jia, X. Lia, Y. Mu, C. Xu, Y. Jiang, X. Yu, J. Wu, and C. Dong, "Coordinated control for EV aggregators and power plants in frequency regulation considering time-varying delays," *Appl. Energy*, vol. 210, pp. 1363-1376, Jan. 2018.

[13] N. Hatziargyriou, *Microgrids: Architecture and Control*, West Sussex: Wiley-IEEE Press, 2014.

[14] R. Zamora and A. K. Srivastava, "Controls for micro-grids with storage: Review, challenges, and research needs," *Renew. Sust. Energ. Rev.*, vol. 14, pp. 2009–2018, Sep. 2010.

[15] P. Kundur, *Power System Stability and Control*, New York: McGraw-Hill, 1994.

[16] X. Li, Y. Song, and S. Han, "Frequency control in micro-grid power system combined with electrolyzer system and fuzzy PI controller," *J. Power Sources*, vol. 180, pp. 468–475, May 2008.

[17] M. Nayeripour, M. Hoseintabar, and T. Niknam, "Frequency deviation control by coordination control of FC and double-layer capacitor in an autonomous hybrid renewable energy power generation system," *Renew. Energ*., vol. 36, pp. 1741-1746, June 2011.

[18] B. S. Kumar and S. Mishra, "AGC for distributed generation," In Proc. *2008 IEEE International Conference on Sustainable Energy Technologies*, pp. 89–94, Singapore, 24-27 Nov. 2008.

[19] M. H. Khooban, "Secondary load frequency control of time-delay stand-alone microgrids with electric vehicles," *IEEE Trans. Ind. Electron*., vol. 65, pp. 7416-7422, September 2018.

[20] A. Kaur, J. Kaushal, and P. Basak, "A review on microgrid central controller," *Renew. Sust. Energ. Rev.*, vol. 55, pp. 338-345, March 2016.

[21] C. A. Macana, E. M. Nava, and N. Quijano, "Time-delay effect on load frequency control for micro-grids," in *Proc. 10th IEEE International Conference on Networking, Sensing and Control (ICNSC)*, pp. 544-549, Evry, France, 27 June 2013.

[22] H. Gündüz, Ş. Sönmez, and S. Ayasun, "Comprehensive gain and phase margins based stability analysis of microgrid frequency control system with constant communication delays," *IET Gener. Transm. Distrib*., vol. 11, pp. 719- 729, Feb. 2017.

[23] A. Khalil, Z. Rajab, A. Alfergani and O. Mohamed "The impact of time delay on load frequency control system in microgrid with plug-in electric vehicles," *Sustain. Cities Soc.*, vol. 35, pp. 365-377, November 2017

[24] M. T. Söylemez, N. Munro, and H. Baki, "Fast calculation of stabilizing PID controller," *Automatica*, vol. 39, pp. 121–126, Jan. 2003.

[25] N. Tan, I. Kaya, C. Yeroglu, and D. P. Atherton, "Computation of stabilizing PI and PID controllers using the stability boundary locus," *Energy Convers. Manag.*, vol. 47, pp. 3045-3058, Nov. 2006.

[26] Simulink, Model-Based and System-Based Design, Using Simulink, MathWorks Inc., Natick, 2000.

APPENDIX

The coefficients of the characteristic equation in (5):

$$
\begin{aligned}
p_6 &= (K_{MT} MT_{ES} T_{FC} T_{EV} + K_{MT} K_{PL} MT_{ES} T_{FC} T_{EV}),\\
p_5 &= (T_{ES} T_{EV} T_{FC} + K_{MT} MT_{ES} T_{EV} + K_{MT} MT_{ES} T_{FC}\\
&\quad + K_{MT} MT_{EV} T_{FC} + DK_{MT} T_{ES} T_{EV} T_{FC}\\
&\quad + K_{MT} K_{PL} MT_{ES} T_{EV} + K_{MT} K_{PL} MT_{ES} T_{FC}\\
&\quad + K_{MT} K_{PL} MT_{EV} T_{FC} + DK_{MT} K_{PL} T_{ES} T_{EV} T_{FC}\\
&\quad + K_{IL} K_{MT} MT_{ES} T_{EV} T_{FC}),
\end{aligned}
$$

$$
\begin{aligned}
p_4 &= (-K_{FC} K_{MT} T_{ES} T_{EV} + T_{ES} T_{FC} + T_{EV} T_{FC}\\
&\quad + K_{MT} MT_{ES} + K_{MT} MT_{EV} + K_{MT} MT_{FC} DK_{MT} T_{ES} T_{EV}\\
&\quad + DK_{MT} T_{ES} T_{FC} + DK_{MT} T_{EV} T_{FC} + K_{MT} K_{PL} MT_{ES}\\
&\quad + K_{MT} K_{PL} MT_{EV} + K_{MT} K_{PL} MT_{FC} + K_{ES} K_{MT} T_{EV} T_{FC}\\
&\quad + T_{ES} T_{EV} + DK_{MT} K_{PL} T_{ES} T_{EV} + DK_{MT} K_{PL} T_{ES} T_{FC}\\
&\quad + DK_{MT} K_{PL} T_{EV} T_{FC} + K_{IL} K_{MT} MT_{ES} T_{EV}\\
&\quad + K_{IL} K_{MT} MT_{ES} T_{FC} + K_{IL} K_{MT} MT_{EV} T_{FC}\\
&\quad + DK_{IL} K_{MT} T_{ES} T_{EV} T_{FC}),
\end{aligned}
$$

$$
\begin{aligned}
p_3 &= (T_{EV} + T_{FC} + K_{MT}M + DK_{MT}T_{ES} + DK_{MT}T_{EV} \\
&\quad + DK_{MT}T_{FC} + K_{MT}K_{PL}M + K_{ES}K_{MT}T_{EV} \\
&\quad + K_{ES}K_{MT}T_{FC} + T_{ES} - K_{FC}K_{MT}T_{EV} - K_{FC}K_{MT}T_{ES} \\
&\quad + DK_{MT}K_{PL}T_{ES} + DK_{MT}K_{PL}T_{EV} + DK_{MT}K_{PL}T_{FC} \\
&\quad + K_{IL}K_{MT}MT_{ES} + K_{IL}K_{MT}MT_{EV} + K_{IL}K_{MT}MT_{FC} \\
&\quad + DK_{IL}K_{MT}T_{ES}T_{EV} + DK_{IL}K_{MT}T_{ES}T_{FC} \\
&\quad + DK_{IL}K_{MT}T_{EV}T_{FC}), \\
p_2 &= (-K_{FC}K_{MT} + K_{ES}K_{MT} + DK_{MT} + DK_{MT}K_{PL} \\
&\quad + K_{IL}K_{MT}M + DK_{IL}K_{MT}T_{ES} + DK_{IL}K_{MT}T_{EV} \\
&\quad + DK_{IL}K_{MT}T_{FC} + 1), \\
p_1 &= (DK_{IL}K_{MT}), \\
q_5 &= (K_{MT}K_{PC}K_{PL}T_{ES}T_{EV}T_{FC}\alpha_0), \\
q_4 &= (K_{EV}K_{MT}K_{PC}T_{ES}T_{FC}\alpha_1 + K_{MT}K_{PC}K_{PL}T_{ES}T_{EV}\alpha_0 \\
&\quad + K_{MT}K_{PC}K_{PL}T_{ES}T_{FC}\alpha_0 + K_{MT}K_{PC}K_{PL}T_{EV}T_{FC}\alpha_0 \\
&\quad + K_{IC}K_{MT}K_{PL}T_{ES}T_{EV}T_{FC}\alpha_0 \\
&\quad + K_{IL}K_{MT}K_{PC}T_{ES}T_{EV}T_{FC}\alpha_0), \\
q_3 &= (K_{EV}K_{MT}K_{PC}T_{ES}\alpha_1 + K_{EV}K_{MT}K_{PC}T_{FC}\alpha_1 + \\
&\quad K_{MT}K_{PC}K_{PL}T_{ES}\alpha_0 + K_{MT}K_{PC}K_{PL}T_{EV}\alpha_0 + \\
&\quad K_{MT}K_{PC}K_{PL}T_{FC}\alpha_0 + K_{EV}K_{IC}K_{MT}T_{ES}T_{FC}\alpha_1 + \\
&\quad K_{IC}K_{MT}K_{PL}T_{ES}T_{EV}\alpha_0 + K_{IL}K_{MT}K_{PC}T_{ES}T_{EV}\alpha_0 + \\
&\quad K_{IC}K_{MT}K_{PL}T_{ES}T_{FC}\alpha_0 + K_{IL}K_{MT}K_{PC}T_{ES}T_{FC}\alpha_0 + \\
&\quad K_{IC}K_{MT}K_{PL}T_{EV}T_{FC}\alpha_0 + K_{IL}K_{MT}K_{PC}T_{EV}T_{FC}\alpha_0 + \\
&\quad K_{IC}K_{IL}K_{MT}T_{ES}T_{EV}T_{FC}\alpha_0), \\
q_2 &= (K_{EV}K_{MT}K_{PC}\alpha_1 + K_{MT}K_{PC}K_{PL}\alpha_0 \\
&\quad + K_{EV}K_{IC}K_{MT}T_{ES}\alpha_1 + K_{EV}K_{IC}K_{MT}T_{FC}\alpha_1 \\
&\quad + K_{IC}K_{MT}K_{PL}T_{ES}\alpha_0 + K_{IL}K_{MT}K_{PC}T_{ES}\alpha_0 \\
&\quad + K_{IC}K_{MT}K_{PL}T_{EV}\alpha_0 + K_{IL}K_{MT}K_{PC}T_{EV}\alpha_0 \\
&\quad + K_{IC}K_{MT}K_{PL}T_{FC}\alpha_0 + K_{IL}K_{MT}K_{PC}T_{FC}\alpha_0 \\
&\quad + K_{IC}K_{IL}K_{MT}T_{ES}T_{EV}\alpha_0 + K_{IC}K_{IL}K_{MT}T_{ES}T_{FC}\alpha_0 \\
&\quad + K_{IC}K_{IL}K_{MT}T_{EV}T_{FC}\alpha_0), \\
q1 &= (K_{EV}K_{IC}K_{MT}\alpha_1 + K_{IC}K_{MT}K_{PL}\alpha_0 \\
&\quad + K_{IL}K_{MT}K_{PC}\alpha_0 + K_{IC}K_{IL}K_{MT}T_{ES}\alpha_0 \\
&\quad + K_{IC}K_{IL}K_{MT}T_{EV}\alpha_0 + K_{IC}K_{IL}K_{MT}T_{FC}\alpha_0), \\
q0 &= (K_{IC}K_{IL}K_{MT}\alpha_0).
\end{aligned}
$$

The coefficients of m and n in (6):

$$
\begin{aligned}
m_5 &= K_{MT}K_{PL}T_{ES}T_{EV}T_{FC}\alpha_0, \\
m_4 &= K_{EV}K_{MT}T_{ES}T_{FC}\alpha_1 + K_{MT}K_{PL}T_{ES}T_{EV}\alpha_0 \\
&\quad + K_{MT}K_{PL}T_{ES}T_{FC}\alpha_0 + K_{MT}K_{PL}T_{EV}T_{FC}\alpha_0 \\
&\quad + K_{MT}K_{IL}T_{ES}T_{EV}T_{FC}\alpha_0, \\
m_3 &= K_{EV}K_{MT}T_{ES}\alpha_1 + K_{EV}K_{MT}T_{FC}\alpha_1 \\
&\quad + K_{MT}K_{PL}T_{ES}\alpha_0 + K_{MT}K_{PL}T_{EV}\alpha_0 \\
&\quad + K_{MT}K_{PL}T_{FC}\alpha_0 + K_{MT}K_{IL}T_{ES}T_{EV}\alpha_0 \\
&\quad + K_{MT}K_{IL}T_{ES}T_{FC}\alpha_0 + K_{MT}K_{IL}T_{EV}T_{FC}\alpha_0, \\
m_2 &= K_{EV}K_{MT}\alpha_1 + K_{MT}K_{PL}\alpha_0 + K_{IL}K_{MT}T_{ES}\alpha_0 \\
&\quad + K_{IL}K_{MT}T_{EV}\alpha_0 + K_{IL}K_{MT}T_{FC}\alpha_0, \\
m_1 &= K_{IL}K_{MT}\alpha_0, \\
n_4 &= K_{MT}K_{PL}T_{ES}T_{EV}T_{FC}\alpha_0, \\
n_3 &= K_{EV}K_{MT}T_{ES}T_{FC}\alpha_1 + K_{MT}K_{PL}T_{ES}T_{EV}\alpha_0 \\
&\quad + K_{MT}K_{PL}T_{ES}T_{FC}\alpha_0 + K_{MT}K_{PL}T_{EV}T_{FC}\alpha_0 \\
&\quad + K_{IL}K_{MT}T_{ES}T_{EV}T_{FC}\alpha_0 \\
n_2 &= K_{EV}K_{MT}T_{ES}\alpha_1 + K_{EV}K_{MT}T_{FC}\alpha_1 \\
&\quad + K_{MT}K_{PL}T_{ES}\alpha_0 + K_{MT}K_{PL}T_{EV}\alpha_0 \\
&\quad + K_{MT}K_{PL}T_{FC}\alpha_0 + K_{IL}K_{MT}T_{ES}T_{EV}\alpha_0 \\
&\quad + K_{IL}K_{MT}T_{ES}T_{FC}\alpha_0 + K_{IL}K_{MT}T_{EV}T_{FC}\alpha_0, \\
n_1 &= K_{EV}K_{MT}\alpha_1 + K_{MT}K_{PL}\alpha_0 + K_{IL}K_{MT}T_{ES}\alpha_0 \\
&\quad + K_{IL}K_{MT}T_{EV}\alpha_0 + K_{IL}K_{MT}T_{FC}\alpha_0, \\
n_0 &= K_{IL}K_{MT}\alpha_0.
\end{aligned}
$$

The expressions for A_1, B_1, C_1, A_2, B_2, and C_2 in (7):

$$
\begin{aligned}
A_1(\omega_c) &= m_4\omega_c{}^4\cos(\omega_c\tau) - m_2\omega_c{}^2\cos(\omega_c\tau)a \\
&\quad + m_5\omega_c{}^5\sin(\omega_c\tau) - m_3\omega_c{}^3\sin(\omega_c\tau) \\
&\quad + m_1\omega_c\sin(\omega_c\tau), \\
B_1(\omega_c) &= n_4\omega_c{}^4\cos(\omega_c\tau) + n_0\cos(\omega_c\tau) \\
&\quad - n_2\omega_c{}^2\cos(\omega_c\tau) - n_3\omega_c{}^3\sin(\omega_c\tau) \\
&\quad + n_1\omega_c\sin(\omega_c\tau), \\
C_1(\omega_c) &= -p_6\omega_c{}^6 + p_4\omega_c{}^4 - p_2\omega_c{}^2, \\
A_2(\omega_c) &= m_5\omega_c{}^5\cos(\omega_c\tau) - m_3\omega_c{}^3\cos(\omega_c\tau) \\
&\quad + m_1\omega_c\cos(\omega_c\tau) - m_4\omega_c{}^4\sin(\omega_c\tau) \\
&\quad + m_2\omega_c{}^2\sin(\omega_c\tau), \\
B_2(\omega_c) &= -n_3\omega_c{}^3\cos(\omega_c\tau) + n_1\omega_c\cos(\omega_c\tau) \\
&\quad - n_4\omega_c{}^4\sin(\omega_c\tau) + n_2\omega_c{}^2\sin(\omega_c\tau) \\
&\quad - n_0\sin(\omega_c\tau), \\
C_2(\omega_c) &= p_5\omega_c{}^5 - p_3\omega_c{}^3 + p_1\omega_c.
\end{aligned}
$$